Jin et al. *Experimental & Molecular Medicine* (2018) 50:67
DOI 10.1038/s12276-018-0096-z

Experimental & Molecular Medicine

ARTICLE Open Access

An anti-EGFR × cotinine bispecific antibody complexed with cotinine-conjugated duocarmycin inhibits growth of EGFR-positive cancer cells with KRAS mutations

Junyeong Jin[1,2], Gunwoo Park[3,6], Jong Bae Park[4,5], Soohyun Kim[1,3], Hyori Kim[1,3,7] and Junho Chung[1,2,3]

Abstract

Antibody-drug conjugates (ADCs) can selectively deliver cytotoxic agents to tumor cells and are frequently more potent than naked antibodies. However, optimization of the conjugation process between antibodies and cytotoxic agents and characterization of ADCs are laborious and time-consuming processes. Here, we describe a novel ADC platform using a tetravalent bispecific antibody that simultaneously binds to the tumor-associated antigen and a hapten conjugated to a cytotoxic agent. We selected cotinine as the hapten because it is not present in biological systems and is inert and nontoxic. We prepared an anti-epidermal growth factor receptor (EGFR) × cotinine bispecific antibody and mixed it with an equimolar amount of cotinine-conjugated duocarmycin to form the ADC. This ADC showed significant in vitro and in vivo antitumor activity against EGFR-positive, cetuximab-refractory lung adenocarcinoma cells with KRAS mutations.

Introduction

Epidermal growth factor receptor (EGFR) is a receptor tyrosine kinase in the ErbB family. EGFR overexpression is frequently observed in various human cancers, including head and neck, colorectal, lung, breast, prostate, kidney, pancreatic, ovarian, brain, and bladder cancers[1]. Two pharmacological approaches for cancer treatment have been used to block EGFR: (1) monoclonal antibodies, including cetuximab (Erbitux), panitumumab (Vectibix), and necitumumab (Portrazza); and (2) small-molecule tyrosine kinase inhibitors, including gefitinib (Iressa), erlotinib (Tarceva), afatinib (Gilotrif), and osimertinib (Tagrisso)[2]. However, mutations in EGFR and its downstream signaling molecules are associated with poor clinical response and resistance to EGFR-targeted therapy[3]. Among these oncogene aberrations, KRAS mutations are one of the most commonly occurring and are found in 25% of non-small cell lung cancers and 39% of colorectal cancers[4]. KRAS mutations play a critical role in primary resistance to EGFR-targeted therapy among EGFR-positive cancers. An effective treatment for EGFR-positive cancers with KRAS mutations is not currently available[5].

Antibody-drug conjugates (ADCs) are monoclonal antibodies crosslinked to cytotoxic agents that can selectively deliver cytotoxic agents to antigen-expressing tumor cells[6]. ADCs have the potential to overcome the therapeutic limitations of both conventional antibodies and nonspecific cytotoxic agents[7]. Two ADCs, brentuximab vedotin (Adcetris) and trastuzumab emtansine (Kadcyla), have been approved by the Food and Drug Administration (FDA) for the treatment of lymphoma and human epidermoid growth factor receptor-2 (Her2)-positive metastatic breast cancer, respectively[8]. More than

Correspondence: Junho Chung (jjhchung@snu.ac.kr)
[1]Department of Biochemistry and Molecular Biology, Seoul National University College of Medicine, Seoul 00380, Republic of Korea
[2]Department of Biomedical Science, Seoul National University College of Medicine, Seoul 00380, Republic of Korea
Full list of author information is available at the end of the article.

40 distinct ADCs, including three EGFR-targeting ADCs, are currently in clinical trials[9].

Conventional conjugation of a small molecule to an antibody uses the ε-amino acid chains of lysine residues or deoxidized interchain disulfide bonds on cysteine residues. Nonspecific conjugations produce heterogeneous mixtures of ADCs, resulting in different drug-to-antibody ratios (DARs) and locations of conjugation sites[10]. This heterogeneity has an impact on the solubility, stability, pharmacokinetics, and batch variations of ADCs[11]. Site-specific conjugation methods using intentionally introduced cysteines, unnatural amino acid residues, or enzymatic conjugation methods have been developed to avoid the heterogeneity of ADCs[12]. In addition, the binding activity, stability, and conjugation efficiency of ADCs are influenced by the conjugation sites[13]. Hence, optimization procedures are required for each individual antibody to identify the best conjugation residues[14]. ADCs require frequent multi-step complex conjugation procedures and sophisticated analyses for validation[15]. The antibodies also differ in their abilities to deliver the cytotoxic agents into the target cells, which might be due to their affinities, epitopes, or differences in their pharmacodynamics and pharmacokinetics. Therefore, the selection of the optimal antibody for conventional ADCs is a laborious process requiring the generation of numerous candidate ADCs.

In this study, we tested a new ADC platform comprising an antitumor-associated antigen × hapten antibody and a hapten-conjugated cytotoxic drug (Fig. 1a). The advantage of this platform is its versatility on both the antibody and cytotoxic drug sides. Once the antibodies and the hapten-conjugated cytotoxic drugs are prepared, different combinations can be achieved by mixing the bispecific antibodies with the hapten-conjugated cytotoxic drugs. To test the feasibility of this platform, we adopted a tetravalent bispecific antibody format, which was reported previously[16], and developed a bispecific antibody reactive to human EGFR and the hapten, cotinine. Cotinine, a major metabolite of nicotine, is an ideal hapten for this purpose[17,18] due to its exogeneity, physiological inertness, and non-toxicity[19]. In addition, the carboxylic groups in carboxycotinine (trans-4-cotinine carboxylic acid) can be easily applied to chemical crosslinking[20]. An anti-cotinine single chain variable fragment (scFv) used throughout this study was reported previously[21]. We adopted the anti-EGFR antibody cetuximab, which was approved for the treatment of metastatic colorectal cancer and head and neck squamous cell carcinoma[22]. We also prepared a bivalent cotinine-conjugated peptide crosslinked with duocarmycin (cotinine-duocarmycin). In in vitro and in vivo experiments, the bispecific antibody and cotinine −duocarmycin complex showed significant antitumor activity on EGFR-positive cetuximab-refractory lung adenocarcinoma with KRAS mutations. We believe that this platform will be useful for screening the optimal antibody, which can be combined with a specific cytotoxic drug. With further preclinical examinations, this form of ADC might be used for the development of novel therapeutic treatments.

Materials and methods

Cell culture

A549 (human lung adenocarcinoma), MCF7, and HCC1419 cells were obtained from the Korean Cell Line Bank (Seoul, Republic of Korea) and grown in RPMI-1640 media (Welgene, Seoul, Republic of Korea). U87MG cells were obtained from the American Type Culture Collection (ATCC) and grown in Dulbecco's modified Eagle's medium (Welgene). Cells were grown in media supplemented with 10% heat-inactivated fetal bovine serum (FBS, Gibco, Grand Island, NY, USA), 100 U/mL penicillin and 100 μg/mL streptomycin at 37 °C in a humidified atmosphere with 5% CO_2.

HEK293F cells (Invitrogen, Carlsbad, CA, USA) were grown in FreeStyle™ 293 expression medium (Gibco) containing 100 U/mL penicillin and 100 μg/mL streptomycin in Erlenmeyer tissue culture flasks with vent caps (Corning Inc., Corning, NY, USA) at 37 °C in a 70% humidified atmosphere with 7% CO_2 in an orbital shaking incubator (Minitron, INFORS HT, Bottmingen, Switzerland) at 135 rpm.

Preparation of bispecific cetuximab × anti-cotinine scFv antibody (ERC6)

For construction of the bispecific cetuximab × anti-cotinine scFv antibody (ERC6) and negative control IgG × anti-cotinine scFv antibody (NCC6) expression vectors, genes encoding the light chain and heavy chain fused with an anti-cotinine single chain variable fragment (scFv) through a linker $(Gly\text{-}Gly\text{-}Gly\text{-}Gly\text{-}Ser)_4$ were chemically synthesized (Genscript, Piscataway, NJ, USA). The restriction sites *Age*I and *Xba*I were inserted at the 5′ and 3′ ends, respectively, of the gene encoding the light chain of cetuximab and the negative control antibody. Additional restriction sites, *Nhe*I and *Bsi*WI, were inserted at the 5′ end of the genes encoding the heavy chain of cetuximab and negative control antibody and at the 3′ end of the genes encoding anti-cotinine scFv, respectively. Light chain and heavy chain/linker/anti-cotinine/scFv were subcloned into the mammalian expression vector designed for secretion of recombinant proteins, as described previously[21].

The expression vectors encoding ERC6 and NCC6 were transfected into HEK293F cells (Invitrogen) using 25-kDa linear polyethyleneimine (Polyscience, Warrington, PA, USA), as reported previously[23]. ERC6 and NCC6 were purified from the culture supernatants by affinity

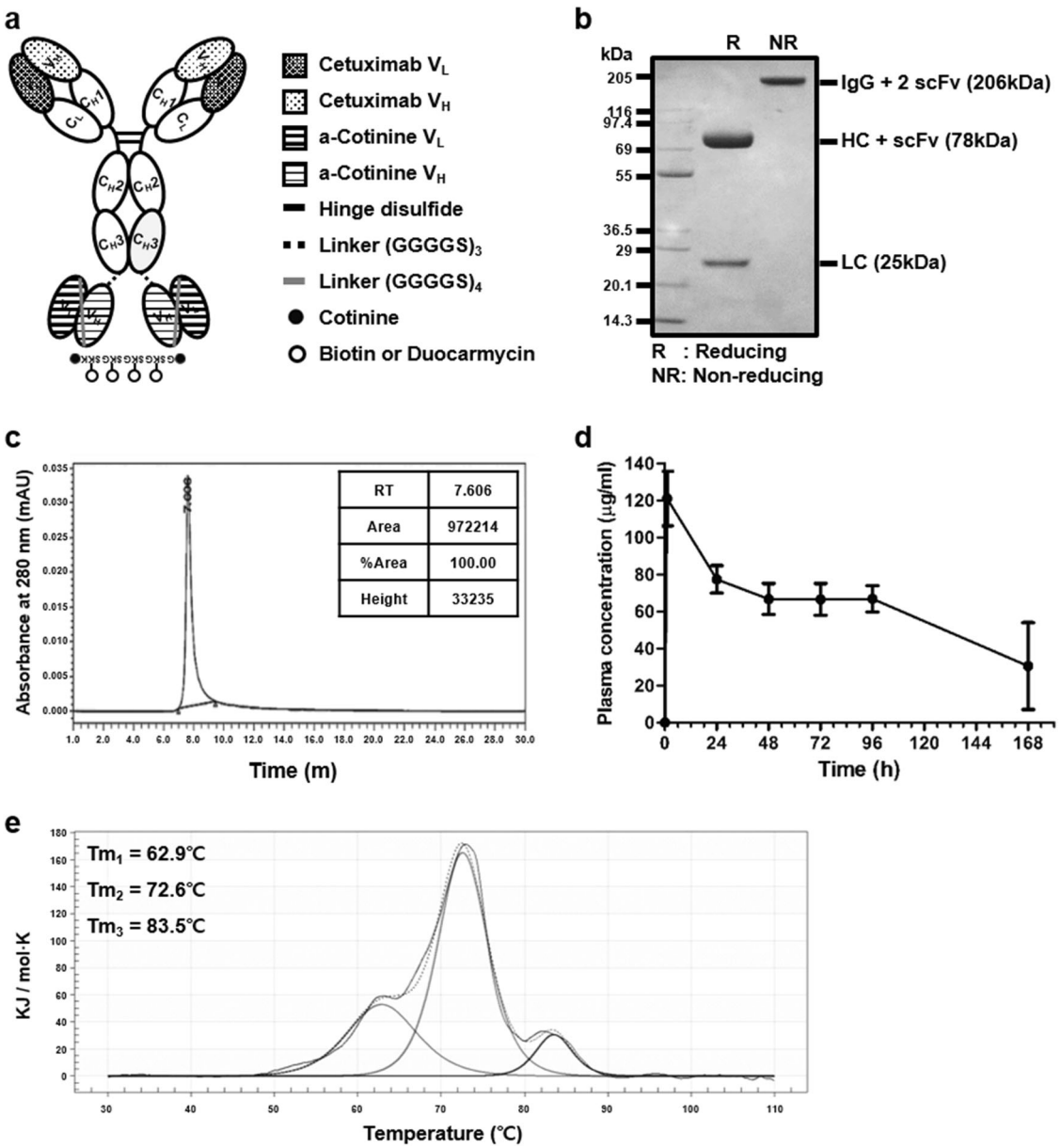

Fig. 1 Generation and characterization of anti-EGFR × cotinine bispecific antibody (ERC6). a A tetravalent bispecific anti-EGFR × cotinine antibody in IgG-HC-scFv of the Morrison format. **b** Purified ERC6 was subjected to 4–12% (w/v) SDS-polyacrylamide gel electrophoresis. The bands were visualized by staining with Coomassie Brilliant Blue R. Lanes 1 and 2 were loaded with and without reducing agent, respectively. **c** Purified ERC6 was subjected to size-exclusion chromatography-high-performance liquid chromatography. **d** ERC6 was intravenously injected into Balb/c mice ($n = 4$), and blood samples were collected via the intraorbital vein. The circulating serum levels of ERC6 were determined via enzyme immunoassays. The results are shown as the mean ± SD acquired from experiments conducted in triplicate. **e** Thermogram of ERC6 by differential scanning calorimetry. *EGFR* epidermal growth factor receptor

chromatography using protein A agarose beads (Repli-Gen, Waltham, MA, USA) as described previously[24].

Sodium dodecyl sulfate-polyacrylamide gel electrophoresis (SDS-PAGE)

Purified ERC6 was resolved by SDS-PAGE using 4–12% NuPage Bis-Tris gels (Invitrogen) according to the manufacturer's instructions. The gels were stained with Coomassie Brilliant Blue R-250 (Amresco, Colon, OH, USA), as described previously[25].

Size-exclusion chromatography (SEC)

Purified ERC6 was analyzed via SEC-HPLC using an Agilent 1260 Infinity high pressure liquid

chromatography (HPLC) system (Agilent Technologies, Santa Clara, CA, USA) equipped with a Bio SEC-3 column (7.8 × 300 mm) that was packed with 3-μm particles of 300 Å pore size (Agilent). The mobile phase contained 50 mM sodium phosphate and 150 mM sodium chloride (pH 7.0). Twenty microliters of ERC6 (1 mg/mL) was injected and eluted isocratically at a flow rate of 1 mL/min for 30 min. The column effluent was monitored by an ultraviolet detector at 280 nm and displayed as mAU. The percentages of monomers, aggregates, and fragments were quantified based on the peak areas[26].

Differential scanning calorimetry (DSC)

Melting temperature was analyzed by nano-DSC (TA Instruments, New Castle, DE, USA). ERC6 at a concentration of 4.85 μM (1 mg/mL) in phosphate-buffered saline (PBS) (pH 7.4) was loaded into the measurement cell, and a DSC thermogram was obtained from 10 °C to 110 °C with a scan rate of 1 °C/min. Data analysis and deconvolution were carried out using NanoAnalyze™ software (TA Instruments), as described previously[27].

Synthesis of cotinine conjugates

All peptides used in this study were chemically synthesized using Fmoc solid phase peptide synthesis techniques (Peptron Inc., Daejon, Republic of Korea). Two trans-4′-cotininecarboxylic acid (Sigma-Aldrich, St Louis, MO, USA) molecules were crosslinked to free amine groups at the N-termini of the GSKGSK, GGGGSKGGGGSK, and GGGSGGGSKGGGSGGGSK peptides (6, 12, and 18 residues, respectively) and at the epsilon amino group of a C-terminal lysine. After elimination of the allyloxycarbonyl (alloc) group on lysine at the middle of the peptides with tetrakis (triphenylphosphine palladium), biotin was conjugated to the free epsilon amine group at lysine. For simplicity, the bivalent cotinine-conjugated peptides crosslinked with biotin are abbreviated as Cot-Biotin-Cot peptide.

Four valine-citrullin p-aminobenzyloxycarbonyl (PAB)-linked dimethylaminoethyl duocarmycins were conjugated to four free amino groups present on four lysines in the bivalent cotinine crosslinked GSKGSKGSKGSKK peptide (Concortis, San Diego, CA, USA). For simplicity, the bivalent cotinine-conjugated peptide crosslinked with four duocarmycins (cotinine-[GSK(duocarmycin)]$_4$K-cotinine) are abbreviated as cotinine-duocarmycin. Cot-Biotin-Cot peptide and cotinine-duocarmycin were purified via reverse-phase HPLC using a C_{18} column. After purification, they were analyzed and validated by mass spectrometry using an Agilent 1100 capillary liquid chromatography and HPLC system (Shimadzu Corp., Kyoto, Japan) equipped with a Capcell Pak C18 column (4.6 × 50 mm, 120 Å) (Shiseido, Tokyo, Japan).

Complexation of cotinine payloads with ERC6

For generation of complexes of cotinine-conjugated payloads with ERC6, cotinine payloads and ERC6 were mixed at equimolar ratios by pipetting. Subsequently, the mixture was incubated for 30 min at room temperature (RT). The complex was then used for in vitro or in vivo assays without further modification.

Enzyme immunoassay (EIA)

The wells of a 96-well microtiter plate (Corning) were coated overnight at 4 °C with human EGFR (Sigma-Aldrich) or bovine serum albumin (BSA)-conjugated cotinine in coating buffer (0.1 M sodium bicarbonate in distilled water, pH 8.6) and blocked with 3% (w/v) BSA in PBS for 1 h at 37 °C. Antibodies at concentrations of 1 μg/mL in 50 μL blocking buffer were added to each well and incubated for 2 h at 37 °C. After washes with 0.05% (v/v) Tween 20 in PBS (PBST), horseradish peroxidase (HRP)-conjugated anti-human IgG (Fab-specific) antibodies (Sigma-Aldrich) diluted in blocking buffer were added and incubated for 1 h at 37 °C. Subsequently, the plates were washed again using 0.05% PBST, followed by adding 50 μL of 3,3′,5,5′-tetramethyl benzidine substrate solution (TMB) (GenDEPOT, Barker, TX, USA) to each well, and the absorbance was measured at 650 nm with a Multiscan Ascent microplate reader (Labsystems, Helsinki, Finland).

For confirmation of the bispecificity of ERC6, human EGFR-coated wells were incubated with antibodies, as described above. After the samples were washed with 0.05% PBST, the Cot-Biotin-Cot peptide was added to each well and incubated for 1 h at 37 °C. HRP-conjugated streptavidin (Thermo Scientific Pierce, Rockford, IL, USA) diluted in blocking buffer was then added and incubated for 1 h at 37 °C. After another wash, TMB was added to each well, and the absorbance at 650 nm was measured.

Pharmacokinetic analyses

All animal experiments conducted in this study were reviewed and approved by the Institutional Animal Care and Use Committee (IACUC) of the National Cancer Center Research Institute, Republic of Korea (Permit number: NCC-15-267). The animals were maintained in the National Cancer Center animal facility in accordance with the AAALAC International Animal Care Policy.

Eight-week-old male Balb/c mice were intravenously injected with 200 μg ERC6 that was preincubated with 964 pmol of Cot-Biotin-Cot peptide at a 1:1 molar ratio dissolved in 100 μL sterile PBS ($n = 4$/group). Blood samples were collected from the intraorbital vein at 0, 1, 24, 48, 72, 96, and 168 h post-injection. The samples were kept at RT for 2 h until the blood coagulated. Subsequently, serum was acquired by centrifugation at 3500 rpm for 15 min at 4 °C. The circulating serum levels of total ERC6 and

ERC6-complexed Cot-Biotin-Cot peptide were determined by EIAs.

Total ERC6 in the serum samples was measured as follows. The wells of a 96-well microtiter plate (Corning) were coated with goat anti-human IgG (Fc-specific) capturing antibody (EMD Millipore, Darmstadt, Germany) in coating buffer overnight at 4 °C and blocked with 3% BSA in PBS. The serum samples diluted in blocking buffer and standard solutions were added to each well and incubated for 2 h at 37 °C. After the samples were washed with 0.05% PBST, HRP-conjugated anti-human C_{kappa} antibody (Chemicon-Millipore, Billerica, MA, USA) diluted in blocking buffer was added and incubated for 1 h at 37 °C. After another wash, TMB (GenDEPOT) was added to each well, and the absorbance at 650 nm was measured.

The complex of ERC6 and the Cot-Biotin-Cot peptide in the serum samples were measured as follows. Human EGFR (Sigma-Aldrich)-coated wells were incubated with serum samples as described above. After washes with 0.05% PBST, HRP-conjugated streptavidin (Thermo Fisher Scientific Pierce, Rockford, IL, USA) was added and incubated for 1 h at 37 °C. After another wash, TMB was added to each well, and the absorbance at 650 nm was measured.

Flow cytometry

A549 cells were seeded into a v-bottom 96-well plate (Corning) with a final density of 4×10^5 cells per well. Cells were treated with either 0 nM or 100 nM of ERC6 and Cot-Biotin-Cot peptide diluted in flow cytometry buffer (1% (w/v) BSA in PBS containing 0.1% (w/v) sodium azide) at 37 °C for 30 min. In the control experiment, negative control IgG, anti-cotinine-IgG, or cetuximab (Erbitux, Merck K GaA, Darmstadt, Germany) was used in place of ERC6. Palivizumab (Synagis; Boehringer Ingelheim Pharma, Biberach a der Riss, Germany) was used as a negative control IgG. After the cells were washed with flow cytometry buffer, they were then incubated with phycoerythrin (PE)-conjugated streptavidin (BD Biosciences Pharminogen, San Diego, CA, USA) and FITC-conjugated anti-human IgG (Fc-specific) antibody (Thermo Fisher Scientific Pierce) for 1 h at 37 °C in the dark. After additional washing with the same buffer, the cells were resuspended in 200 μL PBS and analyzed by flow cytometry using a FACS Canto II instrument (BD Bioscience, San Jose, CA, USA) equipped with a 488-nm laser. We detected 10,000 cells per measurement, and data were analyzed with FlowJo software (TreeStar, Ashland, OR, USA).

Cell viability assays

The effect of ERC6 and cotinine-duocarmycin on tumor cell viability was evaluated using Cell Titer-Glo reagent (Promega Corp., Madison, WI, USA) as described previously[28]. A549, U87MG, MCF7, and HCC1419 cells were seeded in 50 μL of RPMI-1640 medium in black-walled 96-well plates (4000 cells per well) and allowed to adhere overnight at 37 °C in a humidified atmosphere with 5% CO_2. Subsequently, the ERC6 and cotinine−duocarmycin complex was serially diluted tenfold with fresh culture medium (0.02–2000 nM). In the control experiments, negative control IgG, NCC6, or cetuximab (Merck K GaA) was used in place of ERC6. Cotinine-duocarmycin and antibody diluents in 50 μL of medium were added to each well and incubated for 72 h. After addition of Cell Titer-Glo reagent (Promega Corp.) to each well, the luminescence signal was measured using a microplate luminometer (PerkinElmer, Waltham, MA, USA) per the manufacturer's instructions. All experiments were conducted in triplicate. The relative cell viability was calculated by dividing the control luminescent signal [% viability = (Test − Background)/(Control − Background) × 100].

Xenografts

Six-week-old female Balb/c-nude mice were subcutaneously injected with A549 (1×10^7 cells) on the left and right flanks. When the tumor volume reached approximately 150 mm^3, all the animals were randomly divided into three groups ($n = 4$/group) and treated for 5 weeks. Mice were intraperitoneally injected with the drugs twice a week for the first 2 weeks. Group I received negative control IgG (2.15 mg/kg) and cotinine-duocarmycin (95 μg/kg), Group II received ERC6 (3 mg/kg) and dimethylsulfoxide (DMSO), and Group III received the complex of ERC6 (3 mg/kg) and cotinine-duocarmycin (95 μg/kg). Then, the drugs, as stated above, were injected three times a week for the following 3 weeks. Palivizumab was used as a negative control for the bispecific antibody. DMSO was used as a vehicle control for cotinine-duocarmycin. The tumor volume was measured using digital calipers twice a week for 32 days post-injection. Tumor volume was calculated as the length × $(\text{width})^2 \times 0.5$, where length was the longest axis and width was the distance perpendicular to the length, as described previously[29]. Systemic toxicity was evaluated by measuring body weight twice a week. The mice were sacrificed on day 35 post-injection, and the tumors were dissected and weighed.

Immunofluorescence assay

A549 (1×10^7 cells) cells were subcutaneously injected into the left and right flanks of each Balb/c-nude mouse. When the average tumor volume reached 500 mm^3, tumor-bearing mice received a single intraperitoneal (i.p.) injection as follows: Group I received 144 μg of negative control IgG and 1.85 μg of Cot-Biotin-Cot peptide; Group II received 200 μg ERC6 and vehicle (distilled water); and

Group III received a complex of ERC6 (200 μg) and Cot-Biotin-Cot peptide (1.85 μg). Mice were anesthetized with isoflurane and euthanized by transcardial perfusion with 10 mL 4% (w/v) paraformaldehyde in PBS at 24 h post-injection. Dissected tumors were equilibrated in a cryoprotective solution containing 30% (w/v) sucrose in PBS for 24 h at 4 °C and frozen in optimum cutting temperature embedding medium (Sakura Finetek, Torrance, CA, USA) over liquid nitrogen and stored at −80 °C until sectioned, as described previously[30].

For immunofluorescence staining, the cryosections were prepared to a thickness of 4 μm and fixed with 4% paraformaldehyde in PBS for 10 min at RT. After the sections were washed in PBS, they were blocked with 10% (v/v) normal goat serum (CST, Danvers, MA, USA) in IHC-Tek antibody diluent (pH 7.4) (IHC World, Woodstock, MD, USA) for 1 h at RT. The tissue sections were incubated with Alexa Fluor 488-conjugated streptavidin (Molecular Probes Inc., Eugene, OR, USA) for 8 h or stained with Alexa Fluor 594-conjugated anti-human IgG antibody (Molecular Probes) for 16 h in a dark and humidified chamber at 4 °C. After the samples were washed with PBS, nuclei were stained with 4′,6-diamidino-2-phenylindole (DAPI; Pierce, Rockford, IL, USA) according to the manufacturer's instructions. The sections were mounted on slides with fluorescence-mounting medium (DAKO, Glostrup, Denmark), and images were obtained at ×40 magnification using a FV1000 laser scanning microscope (Olympus, Tokyo, Japan) equipped with FV10 ASW software. Emission and excitation filters were arranged to permit simultaneous imaging of three colors.

Statistical analyses

Statistical analyses were performed using GraphPad Prism version 5.0 software (GraphPad Software Inc., San Diego, CA, USA). The results are expressed as the mean ± standard deviation (SD) for the indicated number of independent measurements. Statistical significance was determined using two-tailed unpaired Student's t tests, and p values < 0.05 were considered statistically significant. The p values are indicated in the figures and their legends.

Results

Expression of the bispecific cetuximab × anti-cotinine scFv antibody (ERC6) and characterization

ERC6 was designed in an IgG-based tetravalent bispecific format by fusing anti-cotinine single chain variable fragments (scFvs) to the CH_3 domains of cetuximab (Fig. 1a)[16]. For flexibility, glycine and serine-rich peptide linkers $(Gly\text{-}Gly\text{-}Gly\text{-}Gly\text{-}Ser)_3$ were introduced between the CH_3 domains and the scFv. The gene encoding ERC6 was cloned into a eukaryotic expression vector[18]. ERC6 was purified using protein A affinity column chromatography from transiently transfected HEK393F culture supernatants. The expression yield of the ERC6 was approximately 30 mg/L.

SDS-PAGE was performed to analyze the purity of ERC6. With Coomassie Brilliant Blue R250 staining, the major band with a molecular weight of 206 kDa was visualized in non-reducing conditions, and two major bands at 78 and 25 kDa were observed under reducing conditions (Fig. 1b). The recombinant protein with a molecular weight of 206 kDa corresponded to the fully assembled ERC6, predicted by the ProtParam tool (ExPASy). The 25 and 78 kDa bands matched to the unmodified light chain and heavy chain fused with one scFv on the CH_3 domain of the 78 kDa component.

The physicochemical property of the purified recombinant protein was analyzed by SEC-HPLC. ERC6 was represented as a single major peak with an apparent molecular weight corresponding to the correctly assembled form (Fig. 1c). These data showed that fragments, aggregates, and multimers were not present in the final purified fraction of ERC6.

The thermal stability of ERC6 was analyzed by DSC. The thermogram shows three distinct unfolding transitions with melting temperature (T_m) values of 62.9, 72.6, and 83.5 °C (Fig. 1e). The transition with a T_m of 62.9 °C corresponded to the denaturation of the Fab and scFv (Supplementary Figure 1), and those with T_m values of 72.6 and 83.5 °C were expected to correspond to the denaturation of the CH2 and CH3 domains, respectively[31].

EIA was used to test the reactivity of ERC6 against EGFR and cotinine. ERC6 reacted specifically to EGFR and cotinine-BSA coated on microtiter plates (Fig. 2a). To confirm that ERC6 bound to both human EGFR and cotinine simultaneously, we performed additional EIAs using a streptavidin-biotin detection system. After incubation human EGFR-coated microtiter plates with ERC6, bivalent cotinine-conjugated peptide crosslinked with biotin (Cot-Biotin-Cot peptide) (Fig. 3a) was added to each well followed by the addition of HRP-conjugated streptavidin. In these conditions, ERC6 simultaneously bound to EGFR and cotinine (Fig. 2b).

Pharmacokinetics of the ERC6 and ERC6 complexes

Pharmacokinetic analysis was also performed to assess the in vivo stability of ERC6. The serum half-life of ERC6 was determined in Balb/c mice ($n = 4$). The circulating serum level of ERC6 was determined via EIAs using blood samples collected from the intraorbital vein. After incubation of the serum on the anti-human IgG (Fc-specific) capture antibody-coated plate, the signal was detected by addition of HRP-conjugated anti-human C_{kappa} detection antibody. Intravenously injected ERC6 was stable for up to 5 days in mouse serum ($t_{1/2} = 108$ h) (Fig. 1d), which is

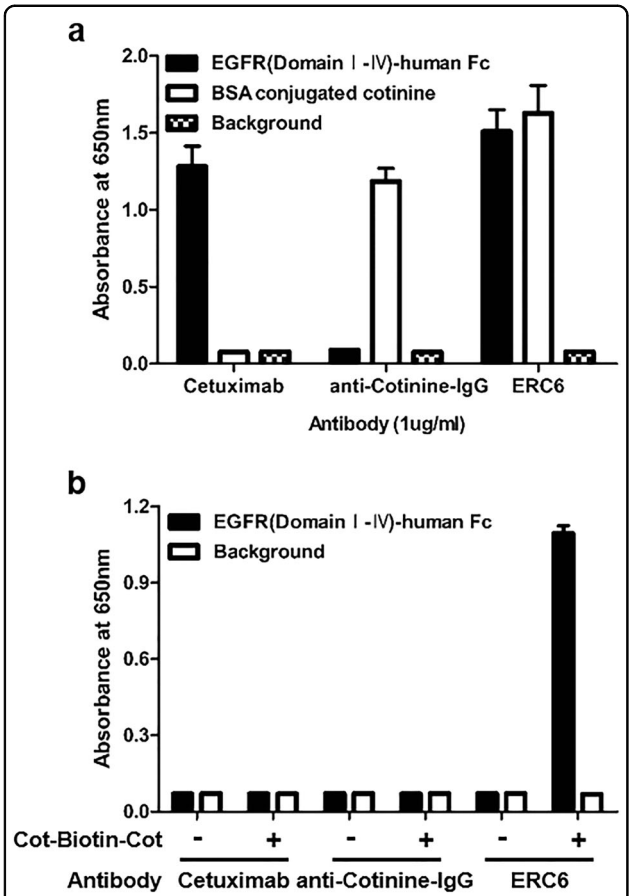

Fig. 2 Reactivity of ERC6 to human EGFR and cotinine. a Cetuximab, anti-cotinine-IgG, and ERC6 were added to wells of a microtiter plate coated with human EGFR (■) or cotinine (□). The wells were probed with HRP-conjugated anti-human IgG (Fab-specific) antibody. **b** Cetuximab, anti-cotinine-IgG, and ERC6 were added to different wells of a microtiter plate coated with human EGFR (■). After addition of Cot-Biotin-Cot peptide, wells were probed with HRP-conjugated streptavidin. The background signal was measured in control wells that were coated with BSA (□). Absorbance at 650 nm was measured. The results are shown as the mean ± SD acquired from experiments conducted in triplicate. EGFR epidermal growth factor receptor, HRP horseradish peroxidase, BSA bovine serum albumin

comparable to that of the cetuximab IgG in the literature[32].

For determination of the in vivo stability of the ERC6 complex and the cotinine-cytotoxic agent, pharmacokinetic analyses were conducted using the Cot-Biotin-Cot peptide. Because we did not know the optimal length of the peptide between the two cotinine molecules, we tested three Cot-Biotin-Cot peptides with different amino acid lengths (6, 12, and 18 amino acid residues) (Fig. 3a). The plasma concentrations of the ERC6 and Cot-Biotin-Cot peptide complexes maintained the highest level when the peptide was 12 amino acids (Fig. 3b), although the plasma levels of ERC6 were not significantly different among the tested groups (Fig. 3c). It is reasonable for the length between two cotinine molecules to affect its binding to ERC6. When the length was too short, it could induce molecular strain in ERC6 after binding. In contrast, the peptide would be kinked if bound to two anti-cotinine scFvs in an ERC6 molecule. This result also demonstrated that the valency was critical for prolonging the half-life of the complex. The half-life of the complex was determined to be approximately 18 h (Fig. 3a), which was significantly longer than that achieved with monovalent binding[33].

ERC6-complexed cotinine-duocarmycin induced potent cytotoxic effects in lung adenocarcinoma cells with KRAS mutations

A549 is a lung adenocarcinoma cell line expressing wild-type EGFR and is resistant to EGFR-targeted therapy because it contains the KRAS mutation. Thus, we used this cell line to test the efficacy of the ERC6-complexed cotinine-cytotoxic agent on cancer cells with wild-type EGFRs and KRAS mutations.

The reactivity of ERC6 to EGFR on the A549 cell surface was confirmed by flow cytometric analyses. ERC6 bound to EGFR expressed on the plasma membrane to a degree similar to that of cetuximab (Fig. 4). The mixture of Cot-Biotin-Cot peptide with either anti-cotinine-IgG or cetuximab did not generate a significant signal attributable to streptavidin-PE.

Cotinine-duocarmycin was prepared by synthesizing a 13-amino acid long peptide with the sequence GSKGSKGSKGSKK, conjugating two cotinines at the N- and C-terminal ends, and crosslinking duocarmycin at the epsilon amino group of four lysine residues (Fig. 5a, b and Supplementary Figure 2a). A valine-citrullin linker was introduced between lysine and duocarmycin, which could be cleaved after endo-lysosomal fusion by cathepsin B to release duocarmycin[34]. The stoichiometry of ERC6 and cotinine-duocarmycin when they formed a complex was evaluated by mass analysis. ERC6-complexed cotinine-duocarmycin existed mostly as a one-to-one complex. Two-to-two and three-to-three complexes were also detected (Supplementary Figure 2c), which might have formed from ERC6 dimers and trimers (Supplementary Figure 2b).

The cytotoxic activity of ERC6-complexed cotinine-duocarmycin against A549 cells was examined. After treatment, the cell viability was determined by measuring the cellular ATP content. The cytotoxicity of ERC6-complexed cotinine-duocarmycin was correlated with the expression level of EGFR (Supplementary Figure 3 and Fig. 5c–f). ERC6-complexed cotinine-duocarmycin showed potent cytotoxic effects against A549 (EGFR+++) and U87MG (EGFR++) cells. The half maximal inhibitory concentration (IC_{50}) on A549 cells was 0.3 nM (Fig. 5c) and that on U87MG cells was 4.0 nM (Fig. 5d). The cytotoxicity of cotinine-duocarmycin was significantly

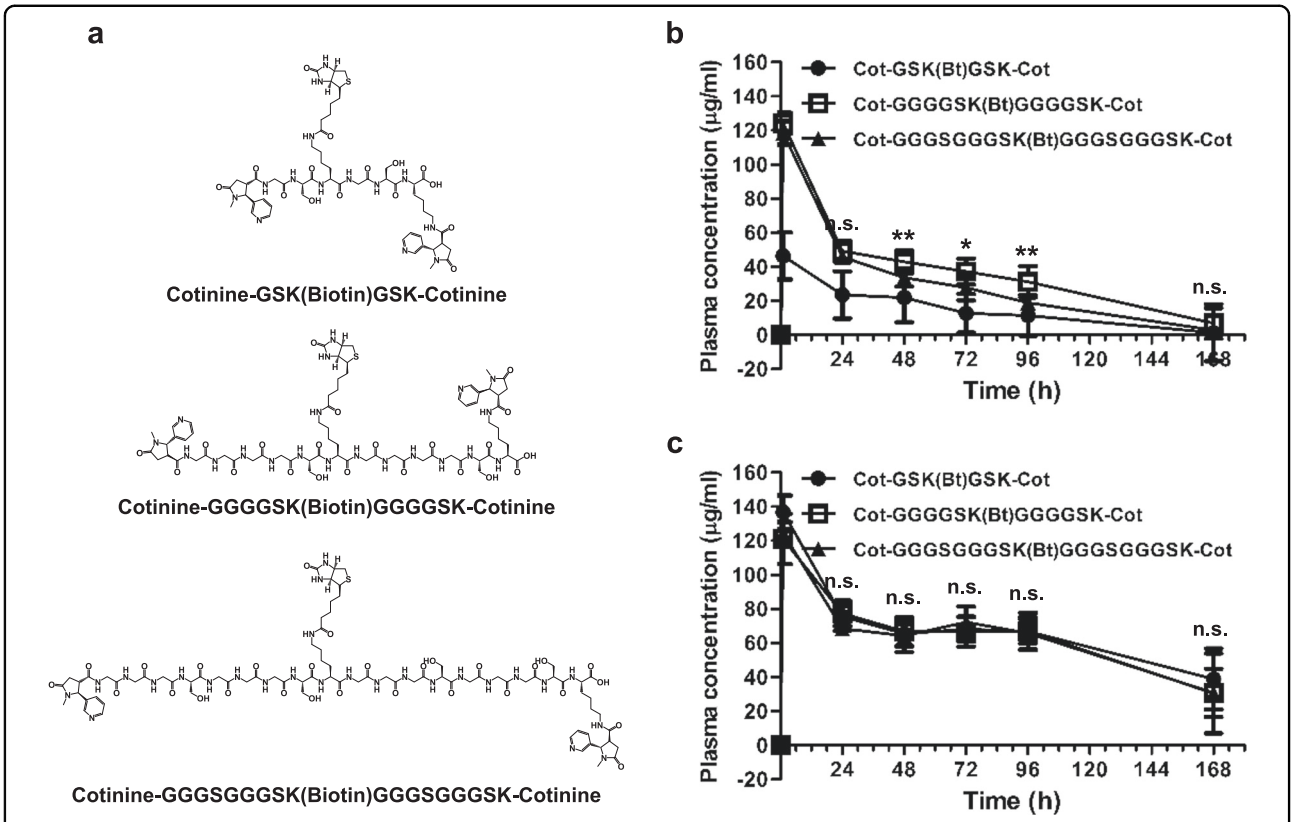

Fig. 3 Pharmacokinetic analysis of ERC6-complexed Cot-Biotin-Cot peptides. a The chemical structure of bivalent cotinine-conjugated peptides with crosslinked biotin (Cot-Biotin-Cot peptide). Cot-Biotin-Cot peptides had different amino acid lengths with 6 (GSKGSK), 12 (GGGGSKGGGGSK), or 18 (GGGSGGGSKGGGSGGGSK) amino acid residues between two cotinine molecules. **b** Pharmacokinetic analysis of ERC6-complexed Cot-Biotin-Cot peptide. Balb/c mice ($n = 4$) were intravenously injected with 200 μg of ERC6 that was preincubated with 964 pmol of Cot-Biotin-Cot peptide at a 1:1 molar ratio dissolved in 100 μL of sterile PBS. Each group was injected with Cot-Biotin-Cot peptides with 6 (●), 12 (□), or 18 (▲) amino acid residues. Blood samples were collected via the intraorbital vein, and the circulating serum levels of ERC6-complexed Cot-Biotin-Cot peptide were determined via enzyme immunoassays (EIAs). **c** Circulating serum levels of total ERC6 were also determined via EIAs. The results are shown as the mean ± SD acquired from experiments conducted in triplicate; $^{*}P < 0.05$, $^{**}P < 0.01$ compared with the group, Student's *t* test. PBS phosphate-buffered saline

reduced when it was mixed with NCC6, cetuximab or negative control IgG. Notably, the cytotoxicity of duocarmycin was dramatically reduced after conjugation to cotinine (Fig. 5c, f and Supplementary Figure 4a, b). Neither ERC6 nor cetuximab inhibited the proliferation of A549 cells significantly because of the primary resistance of A549 cells to EGFR-targeted therapy as previously described (Fig. 5c)[29]. Compared to A549 (EGFR+++) and U87MG (EGFR++) cells, the cytotoxic potency of ERC6-complexed cotinine-duocarmycin on MCF7 (EGFR +) cells was significantly lower, with IC_{50} values of 40 nM (Fig. 5e), and was not strongly influenced by the substitution of ECR6 with NCC6, cetuximab, or a negative control antibody. The IC_{50} value of ERC6-complexed cotinine-duocarmycin on HCC1419 (EGFR-) cells was 100 nM (Fig. 5f), which was equivalent to that of cotinine-duocarmycin mixed with NCC6, ceutixmab, or a negative control antibody. These results demonstrated that ERC6 efficiently enhanced the internalization of cotinine-duocarmycin into the EGFR-positive cells, possibly by receptor-mediated endocytosis.

ERC6-complexed cotinine-duocarmycin inhibited tumor growth in animal models of lung adenocarcinoma

To evaluate the in vivo efficacy of ERC6-complexed cotinine-duocarmycin, we grafted A549 cells into mice ($n = 4$/group). When the tumor volume reached 150 mm^3, mice were intraperitoneally injected with ERC6-complexed cotinine-duocarmycin, a mixture of a negative control IgG and cotinine-duocarmycin, or a mixture of ERC6 and DMSO for 5 weeks. The mice were treated twice a week for the first 2 weeks and then three times a week for the following 3 weeks.

The mice receiving ERC6-complexed cotinine-duocarmycin showed significant growth inhibition of the tumor compared to the other two control groups (Fig. 6a,

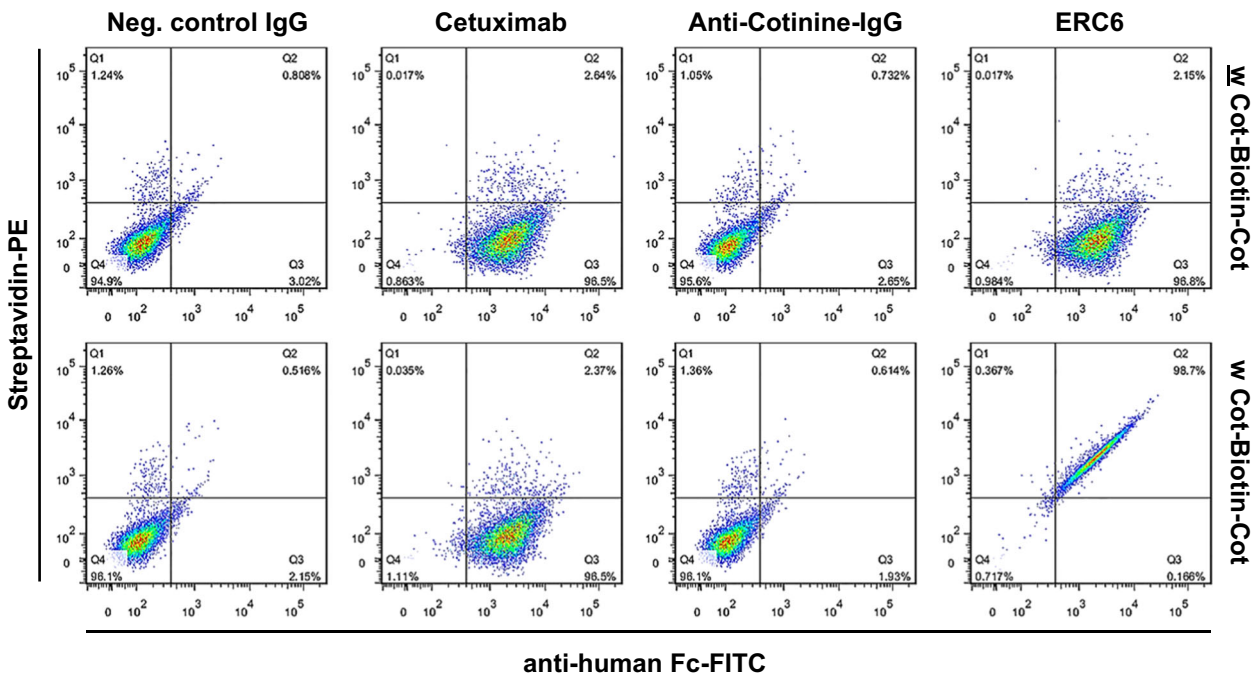

Fig. 4 Flow cytometric analysis of the effects of ERC6-complexed Cot-Biotin-Cot on an EGFR-positive lung adenocarcinoma cell line. A549 cells were incubated with cetuximab, anti-cotinine IgG, ERC6, or negative control IgG (Neg. control IgG) in the absence (w) or presence (w) of Cot-Biotin-Cot peptide. The cells were probed with PE-conjugated streptavidin and FITC-conjugated anti-human Fc for analysis. PE phycoerythrin, FITC fluorescein isothiocyanate

c–e). Although cotinine-duocarmycin showed anti-proliferative effects on A549 in vitro, cotinine-duocarmycin with a negative control IgG did not inhibit the tumor growth in vivo. In this setting, the cotinine-duocarmycin might have been excreted rapidly through the kidney due to its small molecular weight, which could have resulted in insufficient delivery to the tumor tissue. However, ERC6 not only extended the half-life of cotinine-duocarmycin but also specifically delivered it to the EGFR-expressing tumor tissues.

Furthermore, there was no significant weight loss in the mice during the 5-week treatment period (Fig. 6b). This observation suggested that ERC6 and cotinine-duocarmycin did not have systemic toxicity. Taken together, these data showed that ERC6 acted as a drug carrier and selectively delivered cotinine-conjugated cytotoxic drugs to the EGFR-expressing tumor tissues in a target-specific manner without systemic toxicity.

The tissue distribution of ERC6-complexed cotinine payloads in a mouse xenograft tumor model

To examine the specific delivery of the cotinine payloads to the antigen-expressing tumor tissues, immunofluorescence assays were performed on the A549 xenograft mouse model (Fig. 7). Tumor-bearing mice were intraperitoneally injected with ERC6-complexed Cot-Biotin-Cot peptide, a mixture of negative control IgG with Cot-Biotin-Cot peptide, or ERC6 with vehicle. Animals were sacrificed 24 h post-injection, and dissected tumor tissues were subjected to immunohistochemical analyses. The cotinine payloads and antibodies on the tumor tissues were detected by fluorescently labeled secondary antibodies. All the antibodies were detected by Alexa 594-labeled anti-human Fc (red), and the Cot-Biotin-Cot peptide was detected by Alexa 488-labeled streptavidin (green).

Accumulation of ERC6 on human EGFR-positive tumor tissues was observed; however, accumulation of negative control IgG was not observed (Fig. 7, left panel). Furthermore, the intratumoral localization of Cot-Biotin-Cot was observed only when it was injected with ERC6 (Fig. 7c, middle panel). These observations demonstrated that ERC6 selectively delivered cotinine payloads to the tumor site in vivo in a target-specific manner.

Discussion

In this study, we developed a new ADC platform composed of an antitumor-associated antigen × cotinine bispecific antibody and cotinine-cytotoxic agent. One advantage of the system was the ease of selecting an optimal antibody for ADC. For the development of ADCs, it is essential to select antibodies that efficiently

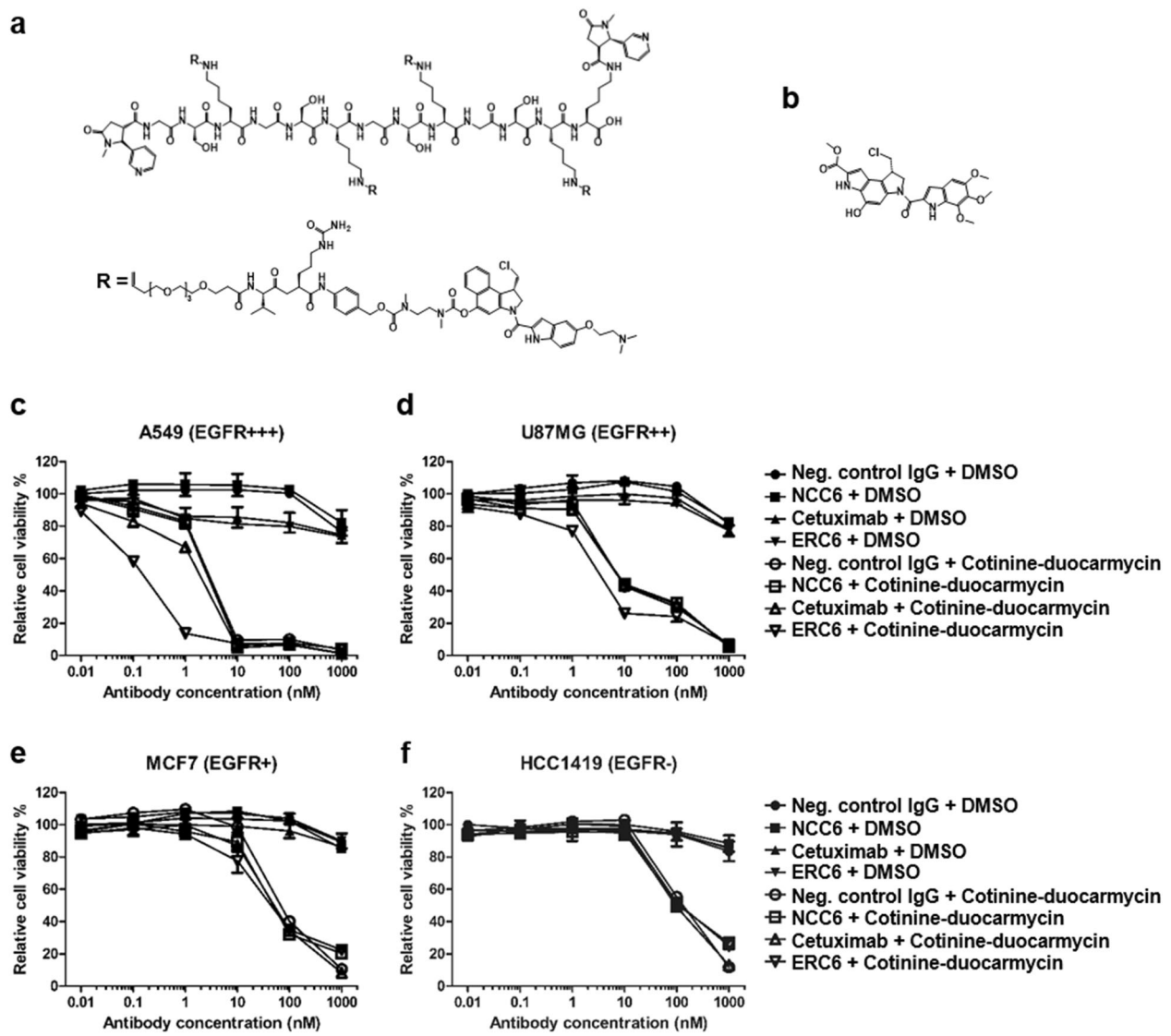

Fig. 5 The anti-proliferative effects of ERC6-complexed cotinine-duocarmycin on an EGFR-positive lung adenocarcinoma cell line. a The chemical structure of bivalent cotinine-conjugated peptide crosslinked with four duocarmycins (cotinine-duocarmycin). R represents valine-citrullin p-aminobenzyloxycarbonyl (PAB)-linked dimethyl aminoethyl duocarmycin. **b** The chemical structure of free duocarmycin. **c** The A549, **d** U87MG, **e** MCF7, and **f** HCC1419 cells were treated with negative control IgG and DMSO (●); negative control IgG × cotinine bispecific antibody (NCC6) and DMSO (■); cetuximab and DMSO (▲); ERC6 and DMSO (▼); negative control IgG and cotinine-duocarmycin (○); NCC6 and cotinine-duocarmycin (□); cetuximab and cotinine-duocarmycin (△); or ERC6 and cotinine-duocarmycin (▽). DMSO was used as a vehicle control for cotinine-duocarmycin. After the cells were incubated for 72 h with the agents, the relative cell viability was determined by measuring the cellular ATP content using the Cell Titer-Glo reagent. The results are shown as the mean ± SD acquired from experiments conducted in triplicate

internalize into cancer cells and release the cytotoxic agents[35]. However, preparation of ADCs requires multi-step conjugation procedures to link a cytotoxic agent to the antibody, and heterogeneous mixtures of ADCs with variable DARs are frequently achieved[11], making the selection process difficult[36]. Our platform technology does not require these conjugation and characterization processes and therefore easily provides comparison data among the antibodies.

We selected a tetravalent bispecific antibody structure for the bispecific antibody. Frequently, bivalent binding of antibodies to receptors on cytoplasmic membranes facilitates better receptor internalization than does monovalent binding[37], and receptor internalization is essential for the cytotoxic effect of ADCs[38]. Four therapeutically available ADCs (gemtuzumab ozogamicin, brentuximab vedotin, trastuzumab emtansine, and inotuzumab ozogamicin) bind to their targets in a bivalent mode, and most

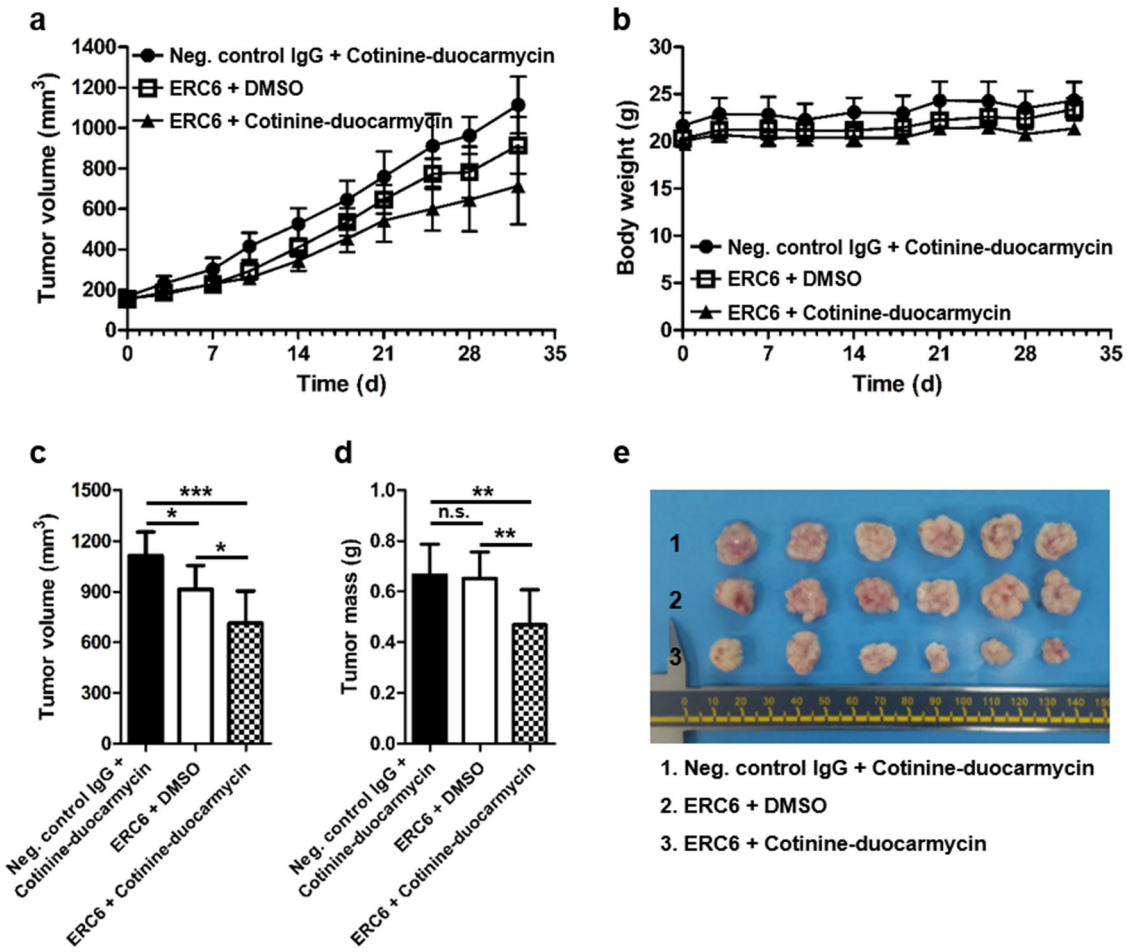

Fig. 6 Efficacy of ERC6-complexed cotinine-duocarmycin in a mouse xenograft tumor model. a The A549 cells were subcutaneously injected into the left and right flanks of Balb/c-nude mice. When the tumor volume reached 150 mm^3, the mice were randomly divided into three groups ($n = 4$/group) and treated for 5 weeks. Each group was intraperitoneally injected with ERC6-complexed cotinine-duocarmycin (▲), ERC6 and DMSO (□) or negative control IgG and cotinine-duocarmycin (●), and the tumor volumes were measured for 32 days. **b** Body weights were monitored during the treatment period. **c** The average tumor volume on day 32. The results are shown as the mean ± SD; $^{*}P < 0.05$, $^{**}P < 0.01$ compared with the group; Student's *t* test. **d** The average dissected tumor mass at sacrifice. **e** Tumor tissues from three treatment groups on day 32

of the ADCs presently under development are also bivalent[36]. We hypothesized that bivalent binding of cotinine-cytotoxic agent to ERC6 would provide much more stability to the complex and extend its in vivo half-life compared to monovalent binding[39,40]. Currently, more than 100 bispecific antibody formats have been proposed[41], and there are only 35 antibody formats providing tetravalent bispecificity[42]. Among these formats, we selected IgG-HC-scFv of the Morrison format, as it is most commonly used[42]. The same format was applied to five antibodies that are currently in clinical development[43]. The distance between the two cotinines affected the in vivo half-life of the complex (Fig. 3b), and the bivalency for cotinine affected the stabilization of the ERC6 and cotinine-duocarmycin complex.

We previously reviewed important factors to consider in selecting a hapten either to be conjugated with an aptamer or isotope-conjugated peptide to extend the in vivo half-life of the aptamer or peptide to be complexed with an antibody for in vivo imaging[18,20,33,44,45]. For these purposes, an optimal hapten should be absent from biological systems, and its pharmacological safety and physiological inertness are essential. Versatile crosslinking to linkers or other compounds is also favored. Histamine-succinyl-glycine, diethylenetriamine pentaacetic acid (DTPA), and 1,4,7,10-tetraazacyclododecane-1,4,7,10-tetraacetic acid (DOTA) have been classically used[46–48]. Recently, we proposed cotinine as an ideal hapten[45]. It is a small chemical with a molecular weight of 176.22 and is a major metabolite of nicotine. It is commonly used as a biomarker for smoking exposure and is absent in human

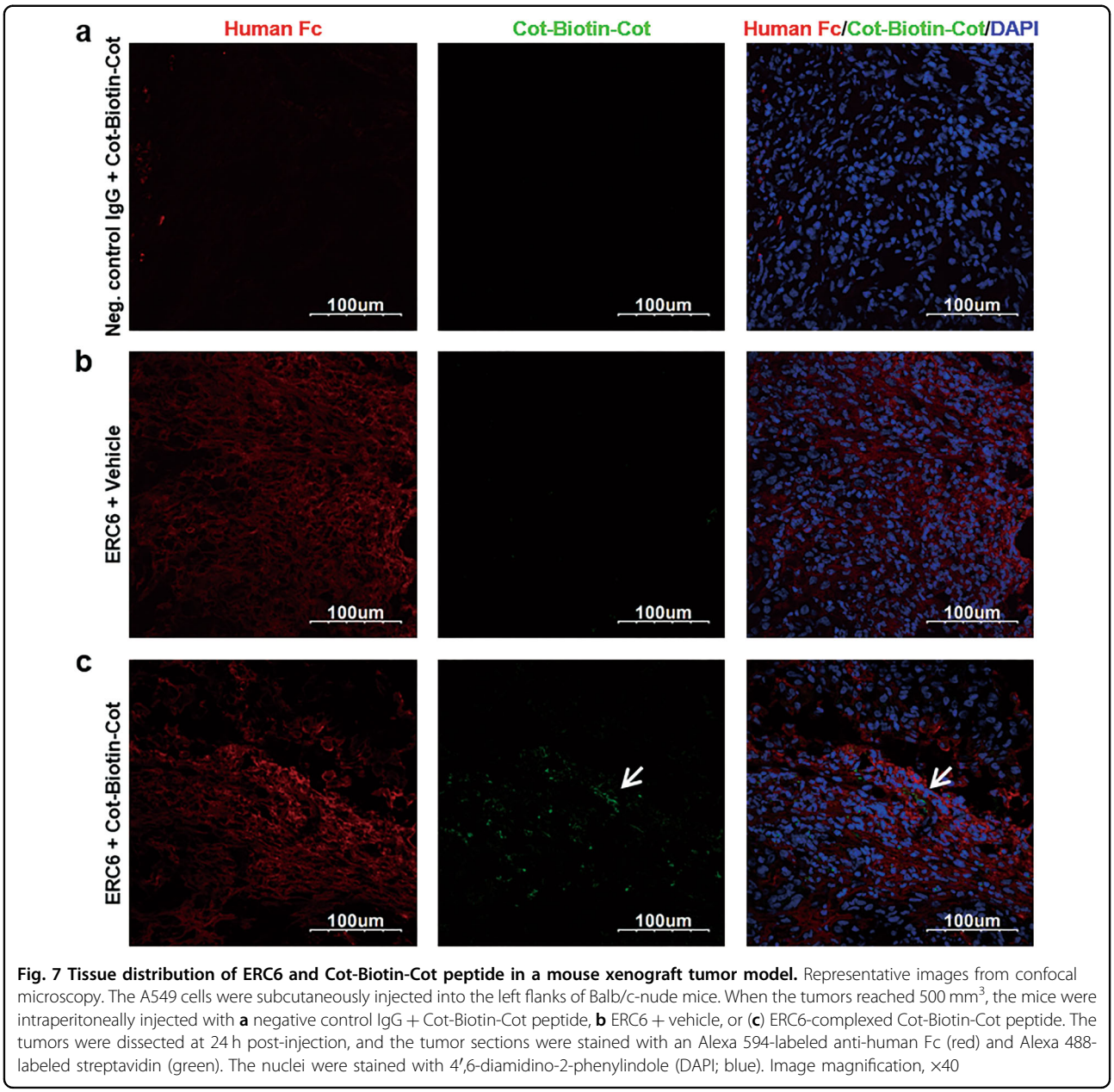

Fig. 7 Tissue distribution of ERC6 and Cot-Biotin-Cot peptide in a mouse xenograft tumor model. Representative images from confocal microscopy. The A549 cells were subcutaneously injected into the left flanks of Balb/c-nude mice. When the tumors reached 500 mm^3, the mice were intraperitoneally injected with **a** negative control IgG + Cot-Biotin-Cot peptide, **b** ERC6 + vehicle, or (**c**) ERC6-complexed Cot-Biotin-Cot peptide. The tumors were dissected at 24 h post-injection, and the tumor sections were stained with an Alexa 594-labeled anti-human Fc (red) and Alexa 488-labeled streptavidin (green). The nuclei were stained with 4′,6-diamidino-2-phenylindole (DAPI; blue). Image magnification, ×40

or animal tissues[17]. Cotinine is nontoxic, with an LD_{50} of 4 ± 0.1 g/kg in mice[19]. No deleterious side effects were induced in humans treated with up to 1800 mg cotinine daily for 4 consecutive days. Carboxycotinine (trans-4-cotininecarboxylic acid) is commercially available at a reasonable cost, and this carboxyl group can be conveniently employed for chemical crosslinking. No immune responses to cotinine have been reported. However, for the purpose of developing an antibody conjugated with cytotoxic agents, a compound with some toxicity might be more beneficial. A high-affinity anti-cotinine antibody was originally generated by our group with k_{on}, k_{off}, and K_D values of $2.6\times10^6\,M^{-1}\times s^{-1}$, $1.3\times10^{-5}\,s^{-1}$, and 4.9×10^{-12} M, respectively[45]. This antibody binds specifically to cotinine and does not cross-react with chemicals with similar structures, such as nicotine, anabasine, caffeine, or cholesterol. This antibody was also confirmed to retain its reactivity in various formats other than as a conventional IgG, such as scFv[20,24].

In this study, ERC6, a cetuximab fused with anti-cotinine scFv at the C-terminus of the heavy chain of the antibody, could be produced with reasonable efficiency and was found to be stable in vitro and in vivo (Fig. 1)[16]. We have synthesized cotinine-conjugated duocarmycin and mixed it with equimolar amounts of ERC6 to form a complex. This complex behaved similar to an ADC

in vitro and in vivo (Fig. 1a). ERC6-complexed cotinine-duocarmycin significantly inhibited tumor growth in the EGFR-positive cetuximab-refractory lung adenocarcinoma with the KRAS mutation both in vitro and in vivo. Its cytotoxic potency was dependent on the expression level of EFGR on the cell surface (Supplementary Figure 3 and Fig. 5c–f). To test whether shuffling of the cytotoxic agents was possible, we also synthesized the cotinine-DM1 conjugate and tested its efficacy in vitro (Supplementary Figure 5), which showed that it was less efficacious than cotinine-duocarmycin.

Cells in epithelial tissue display a relatively high number of EGFR molecules on their surface[49–51]. Therefore, ERC6-complexed cotinine-duocarmycin might exert a cytotoxic effect on EGFR-expressing epithelial cells. We tested this hypothesis using MCF10A, a human normal epithelial cell line, and confirmed that ERC6-complexed cotinine-duocarmycin is indeed cytotoxic to these cells, with an IC_{50} value of 2.0 nM (Supplementary Figures 3 and 6).

Because the cotinine-cytotoxic agents were attached to ERC6 by non-covalent bonds, it was possible for the cotinine-cytotoxic agents to be released from ERC6, which was not observed with conventional ADCs with covalently linked cytotoxic agents. However, the conjugation of cotinine lowered the toxicity of duocarmycin by decreasing its uptake into cells through the cytoplasmic membrane in in vitro experiments (Fig. 5c, e and Supplementary Figure 4a, b). In our in vivo experiments, cotinine-duocarmycin mixed with negative-control IgG did not induce weight loss in mice (Fig. 6b), although duocarmycin has been previously reported to induce significant weight loss in mice[52]. A rapid clearance of liberated cotinine-duocarmycin from the bloodstream could minimize systemic exposure.

In summary, our research suggests that tetravalent bispecific antibodies that simultaneously bind to tumor-associated antigens and cotinine could potentially be used as drug carriers for selective delivery of cotinine-conjugated cytotoxic agents to the antigen-expressing tumor sites.

Acknowledgements
This work was supported by the Bio & Medical Technology Development Program of the National Research Foundation (NRF) funded by the Korean government (MSIP) (grant no. 2014 M3A9D3034034). Junyeong Jin received a scholarship from the BK21-plus education program.

Author details
[1]Department of Biochemistry and Molecular Biology, Seoul National University College of Medicine, Seoul 00380, Republic of Korea. [2]Department of Biomedical Science, Seoul National University College of Medicine, Seoul 00380, Republic of Korea. [3]Cancer Research Institute, Seoul National University College of Medicine, Seoul 00380, Republic of Korea. [4]Research Institute, National Cancer Center, 323 Ilsan-ro, Ilsandong-gu, Goyang 10408, Republic of Korea. [5]Department of Cancer Biomedical Science, National Cancer Center, Graduate School of Cancer Science and Policy, 323 Ilsan-ro, Ilsandong-gu, Goyang 10408, Republic of Korea. [6]Present address: Research Institute, National Cancer Center, 323 Ilsan-ro, Ilsandong-gu, Goyang 10408, Republic of Korea. [7]Present address: Asan Institute for Life Sciences, Asan Medical Center, 88, Olympic-ro 43-gil, Songpa-gu, Seoul 05505, Republic of Korea

Conflict of interest
The authors declare that they have no conflict of interest.

Supplementary information accompanies this paper at https://doi.org/10.1038/s12276-018-0096-z.

Received: 21 August 2017 Revised: 10 March 2018 Accepted: 16 March 2018.
Published online: 24 May 2018

References
1. Mendelsohn, J. & Baselga, J. The EGF receptor family as targets for cancer therapy. *Oncogene* **19**, 6550–6565 (2000).
2. Le, A. D., Alzghari, S. K., Jean, G. W. & La-Beck, N. M. Update on targeted therapies for advanced non-small cell lung cancer: nivolumab in context. *Ther. Clin. Risk Manag.* **13**, 223–236 (2017).
3. Sequist, L. V. et al. Response to treatment and survival of patients with non-small cell lung cancer undergoing somatic EGFR mutation testing. *Oncologist* **12**, 90–98 (2007).
4. Maus, M. K. et al. KRAS mutations in non-small-cell lung cancer and colorectal cancer: implications for EGFR-targeted therapies. *Lung Cancer* **83**, 163–167 (2014).
5. Califano, R., Landi, L. & Cappuzzo, F. Prognostic and predictive value of K-RAS mutations in non-small cell lung cancer. *Drugs* **72**, 28–36 (2012).
6. Liu, R., Wang, R. E. & Wang, F. Antibody-drug conjugates for non-oncological indications. *Expert Opin. Biol. Ther.* **16**, 591–593 (2016).
7. Weiner, G. J. Building better monoclonal antibody-based therapeutics. *Nat. Rev. Cancer* **15**, 361–370 (2015).
8. Kamath, A. V. & Iyer, S. Preclinical pharmacokinetic considerations for the development of antibody drug conjugates. *Pharm. Res.* **32**, 3470–3479 (2015).
9. Polakis, P. Antibody drug conjugates for cancer therapy. *Pharmacol. Rev.* **68**, 3–19 (2016).
10. Diamantis, N. & Banerji, U. Antibody-drug conjugates-an emerging class of cancer treatment. *Br. J. Cancer* **114**, 362–367 (2016).
11. Boylan, N. J. et al. Conjugation site heterogeneity causes variable electrostatic properties in Fc conjugates. *Bioconjug. Chem.* **24**, 1008–1016 (2013).
12. Panowski, S., Bhakta, S., Raab, H., Polakis, P. & Junutula, J. R. Site-specific antibody drug conjugates for cancer therapy. *MAbs* **6**, 34–45 (2014).
13. Behrens, C. R. et al. Antibody-drug conjugates (ADCs) derived from interchain cysteine cross-linking demonstrate improved homogeneity and other pharmacological properties over conventional heterogeneous ADCs. *Mol. Pharm.* **12**, 3986–3998 (2015).
14. Behrens, C. R. & Liu, B. Methods for site-specific drug conjugation to antibodies. *MAbs* **6**, 46–53 (2014).
15. Perez, H. L. et al. Antibody-drug conjugates: current status and future directions. *Drug Discov. Today* **19**, 869–881 (2014).
16. Coloma, M. J. & Morrison, S. L. Design and production of novel tetravalent bispecific antibodies. *Nat. Biotechnol.* **15**, 159–163 (1997).
17. Kim, I. & Huestis, M. A. A validated method for the determination of nicotine, cotinine, trans-3′-hydroxycotinine, and norcotinine in human plasma using solid-phase extraction and liquid chromatography-atmospheric pressure chemical ionization-mass spectrometry. *J. Mass Spectrom.* **41**, 815–821 (2006).
18. Park, S., Hwang, D. & Chung, J. Cotinine-conjugated aptamer/anti-cotinine antibody complexes as a novel affinity unit for use in biological assays. *Exp. Mol. Med* **44**, 554–561 (2012).
19. Riah, O. et al. Evidence that nicotine acetylcholine receptors are not the main targets of cotinine toxicity. *Toxicol. Lett.* **109**, 21–29 (1999).
20. Yoon, S. et al. Bispecific Her2 x cotinine antibody in combination with cotinine-(histidine)2-iodine for the pre-targeting of Her2-positive breast cancer xenografts. *J. Cancer Res. Clin. Oncol.* **140**, 227–233 (2014).

21. Park, S., Lee, D. H., Park, J. G., Lee, Y. T. & Chung, J. A sensitive enzyme immunoassay for measuring cotinine in passive smokers. *Clin. Chim. Acta* **411**, 1238–1242 (2010).
22. Merlano, M. & Occelli, M. Review of cetuximab in the treatment of squamous cell carcinoma of the head and neck. *Ther. Clin. Risk Manag.* **3**, 871–876 (2007).
23. Boussif, O. et al. A versatile vector for gene and oligonucleotide transfer into cells in culture and *in vivo*: polyethylenimine. *Proc. Natl. Acad. Sci. USA* **92**, 7297–7301 (1995).
24. Kim, H., Park, S., Lee, H. K. & Chung, J. Application of bispecific antibody against antigen and hapten for immunodetection and immunopurification. *Exp. Mol. Med.* **45**, e43 (2013).
25. Diezel, W., Kopperschlager, G. & Hofmann, E. An improved procedure for protein staining in polyacrylamide gels with a new type of Coomassie Brilliant Blue. *Anal. Biochem.* **48**, 617–620 (1972).
26. Hong, P., Koza, S. & Bouvier, E. S. Size-exclusion chromatography for the analysis of protein biotherapeutics and their aggregates. *J. Liq. Chromatogr. Relat. Technol.* **35**, 2923–2950 (2012).
27. Gill, P., Moghadam, T. T. & Ranjbar, B. Differential scanning calorimetry techniques: applications in biology and nanoscience. *J. Biomol. Tech.* **21**, 167–193 (2010).
28. Lewis Phillips, G. D. et al. Targeting HER2-positive breast cancer with trastuzumab-DM1, an antibody-cytotoxic drug conjugate. *Cancer Res.* **68**, 9280–9290 (2008).
29. Hsu, Y. F. et al. Complement activation mediates cetuximab inhibition of non-small cell lung cancer tumor growth *in vivo*. *Mol. Cancer* **9**, 139 (2010).
30. Lee, C. M. & Tannock, I. F. The distribution of the therapeutic monoclonal antibodies cetuximab and trastuzumab within solid tumors. *BMC Cancer* **10**, 255 (2010).
31. Strop, P. et al. Generating bispecific human IgG1 and IgG2 antibodies from any antibody pair. *J. Mol. Biol.* **420**, 204–219 (2012).
32. Boross, P. et al. IgA EGFR antibodies mediate tumour killing *in vivo*. *EMBO Mol. Med.* **5**, 1213–1226 (2013).
33. Heo, K. et al. An aptamer-antibody complex (oligobody) as a novel delivery platform for targeted cancer therapies. *J. Control Release* **229**, 1–9 (2016).
34. Srinivasarao, M., Galliford, C. V. & Low, P. S. Principles in the design of ligand-targeted cancer therapeutics and imaging agents. *Nat. Rev. Drug Discov.* **14**, 203–219 (2015).
35. Metz, S. et al. Bispecific digoxigenin-binding antibodies for targeted payload delivery. *Proc. Natl. Acad. Sci. USA* **108**, 8194–8199 (2011).
36. Beck, A., Goetsch, L., Dumontet, C. & Corvaia, N. Strategies and challenges for the next generation of antibody-drug conjugates. *Nat. Rev. Drug Discov.* **16**, 315–337 (2017).
37. Fan, Z., Lu, Y., Wu, X. & Mendelsohn, J. Antibody-induced epidermal growth factor receptor dimerization mediates inhibition of autocrine proliferation of A431 squamous carcinoma cells. *J. Biol. Chem.* **269**, 27595–27602 (1994).
38. Nath, N. et al. Homogeneous plate based antibody internalization assay using pH sensor fluorescent dye. *J. Immunol. Methods* **431**, 11–21 (2016).
39. Rudnick, S. I. & Adams, G. P. Affinity and avidity in antibody-based tumor targeting. *Cancer Biother. Radiopharm.* **24**, 155–161 (2009).
40. Trivedi, A. et al. Clinical pharmacology and translational aspects of bispecific antibodies. *Clin. Transl. Sci.* **10**, 147–162 (2017).
41. Zhang, X., Yang, Y., Fan, D. & Xiong, D. The development of bispecific antibodies and their applications in tumor immune escape. *Exp. Hematol. Oncol.* **6**, 12 (2017).
42. Brinkmann, U. & Kontermann, R. E. The making of bispecific antibodies. *MAbs* **9**, 182–212 (2017).
43. Fan, G., Wang, Z., Hao, M. & Li, J. Bispecific antibodies and their applications. *J. Hematol. Oncol.* **8**, 130 (2015).
44. Park, S. et al. A novel delivery platform for therapeutic peptides. *Biochem. Biophys. Res. Commun.* **450**, 13–18 (2014).
45. Kim, H., Yoon, S. & Chung, J. *In vitro* and *in vivo* application of anti-cotinine antibody and cotinine-conjugated compounds. *BMB Rep.* **47**, 130–134 (2014).
46. Rossi, E. A. et al. Stably tethered multifunctional structures of defined composition made by the dock and lock method for use in cancer targeting. *Proc. Natl. Acad. Sci. USA* **103**, 6841–6846 (2006).
47. Goldenberg, D. M., Rossi, E. A., Sharkey, R. M., McBride, W. J. & Chang, C. H. Multifunctional antibodies by the dock-and-lock method for improved cancer imaging and therapy by pretargeting. *J. Nucl. Med.* **49**, 158–163 (2008).
48. Chang, C. H., Rossi, E. A. & Goldenberg, D. M. The dock and lock method: a novel platform technology for building multivalent, multifunctional structures of defined composition with retained bioactivity. *Clin. Cancer Res.* **13**, 5586s–5591s (2007).
49. Yang, Y. et al. Preclinical studies of a pro-antibody-drug conjugate designed to selectively target EGFR-overexpressing tumors with improved therapeutic efficacy. *MAbs* **8**, 405–413 (2016).
50. Phillips, A. C. et al. ABT-414, an antibody-drug conjugate targeting a tumor-selective EGFR epitope. *Mol. Cancer Ther.* **15**, 661–669 (2016).
51. Donaghy, H. Effects of antibody, drug and linker on the preclinical and clinical toxicities of antibody-drug conjugates. *MAbs* **8**, 659–671 (2016).
52. Vielhauer, G. A. et al. Evaluation of a reductively activated duocarmycin prodrug against murine and human solid cancers. *Cancer Biol. Ther.* **14**, 527–536 (2013).